Appl. Phys. 9, 19—34 (1976)

Applied Physics

Isotope Separation by Laser Deflection of an Atomic Beam*

*Anthony F. Bernhardt***

University of California, Lawrence Livermore Laboratory, Livermore, CA 94550, USA

Received 15 May 1975/Revised 7 October 1975

Abstract. Separation of isotopes of barium has been accomplished by laser deflection of a single isotopic component of an atomic beam. With a tunable narrow linewidth dye laser, small differences in absorption frequency of different barium isotopes on the $6s^2\ ^1S_0$-$6s6p\ ^1P_1$ 5536 Å resonance were exploited to deflect atoms of a single isotopic component of an atomic beam through an angle large enough to physically separate them from the atomic beam.

It is shown that the principal limitation on separation efficiency, the fraction of the desired isotopic component which can be separated, is determined by the branching ratio from the excited state into metastable states. In barium, repeated absorptions and emissions on the 5536 Å transition eventually result in decay from the $6s6p\ ^1P_1$ state to the metastable $6s5d\ ^1D_2$ state. This was observed to occur for all but 3% of the ^{138}Ba atoms. As a result, the efficiency of separation was about 0.7 for the 8 mrad atomic beam divergence employed. (Throughput was nearly 1 mg/day. No attempt was made to maximize this value.)

The isotopic purity of the separated atoms was measured to be in excess of 0.9, limited only by instrumental uncertainty. The effects of near resonant atomic scattering and excitation exchange on isotopic purity are considered.

1. Photodeflection Isotope Separation

The photodeflection method of isotope separation relies on momentum transfer from a directed monochromatic light source to the one isotopic component of an atomic beam which is to be separated from other isotopic components of the beam [1, 2]. When an atom absorbs a photon of energy $h\nu$ it acquires a momentum $h\nu/c$ in the direction of the photon propagation. If the atom decays spontaneously, it will give up momentum $h\nu/c$ to the departing photon in the direction of its propagation. Since an atom is as likely to spontaneously radiate in one direction as it is to radiate in any other direction, the average momentum transfer from N emission events is zero (with a scatter about this value of $h\nu/c\sqrt{N}$) whereas, contributions from the absorption process with a directed light source sum.

The isotopic selectivity of the photodeflection isotope separation process derives from the fact that different isotopes absorb light at slightly different frequencies. Thus a given electronic transition will occur in one isotope at a given frequency and at a slightly different frequency in another. The difference in absorption frequency peaks is designated the isotope shift for the given pair of isotopes considered. The isotope shift is usually large compared to the natural linewidth of the transition. If isotope shifts were much smaller than the natural linewidth, the isotopes could not be distinguished optically except under special circumstances [3] and would not be separable by photodeflection.

In atoms, radiative lifetimes on optical and UV transitions are generally greater than 3×10^{-9} sec so that natural linewidths are less than 5×10^7 Hz. Isotope

* Work performed under the auspices of the U.S. Energy Research & Development Administration.

** Also Fannie & John Hertz Foundation Fellow at the Department of Applied Science, University of California at Davis-Livermore.

shifts are almost always much larger. For light elements the isotope shift is the result of the fact that the reduced masses of the isotopes are different [4]. For a hydrogen-like atom

$$E_a = -\mu_a \frac{e^4}{2\hbar^2 n^2},$$

where μ_a is the reduced mass of isotope a. Since $\mu_a \sim m_e\left(1-\frac{m_e}{M_a}\right)$, where m_e is the electron mass and M_a is the nuclear mass, the energy level is displaced toward the continuum for finite nuclear mass. The displacement is larger for the lighter isotope. The difference in transition energy for two isotopes is

$$h\nu_b - h\nu_a = (\mu_b - \mu_a)\frac{e^4}{2\hbar^2}\left(\frac{1}{n_2^2}-\frac{1}{n_1^2}\right) \simeq \frac{M_b - M_a}{M_b M_a}\frac{m_e e^4}{2\hbar^2}.$$

From these considerations it is seen that the magnitude of the shift in a hydrogen-like atom is given by $\Delta\nu \sim (m_e/m_p)[(A_b - A_a)/A_a A_b]\nu$, where A is the atomic weight, so that $\Delta\nu \sim 5\times 10^{-4}\,\nu/A^2$. This so called "normal mass effect" is characterized by the fact that the lighter isotope transition is less energetic than the heavy isotope transition ($\mu_b > \mu_a \rightarrow \nu_b > \nu_a$) and that the magnitude of the energy difference is inversely proportional to the square of the atomic weight.

For atoms which have more than one electron outside of a closed shell, the mass dependent isotope shift can become more complicated. Consider, for example, an atom with two electrons. The kinetic energy of the system is

$$\frac{P_n^2}{2M} + \frac{1}{2m_e}(P_1^2 + P_2^2),$$

where M and P_n are the mass and momentum of the nucleus. P_1 and P_2 are the momenta of the two electrons. In the center of mass system, the total momentum is zero so that

$$\boldsymbol{P}_n = -(\boldsymbol{P}_1 + \boldsymbol{P}_2) \quad \text{and} \quad P_n^2 = P_1^2 + P_2^2 + 2\boldsymbol{P}_1 \cdot \boldsymbol{P}_2 .$$

The kinetic energy can then be expressed as

$$\frac{1}{2\mu}(P_1^2 + P_2^2) + \frac{1}{M}\boldsymbol{P}_1 \cdot \boldsymbol{P}_2 .$$

The first term gives rise to the "normal mass effect" discussed above while the second term is new. It gives rise to what is referred to as the "specific mass effect". The property of the specific mass effect which is most apparent is that it can have either sign. For $\boldsymbol{P}_1$ parallel to $\boldsymbol{P}_2$ (on the average) it is positive. For opposed motions (on the average) the term has a negative sign. A quantum mechanical treatment of the problem [5] shows that the positive sign applies to singlet terms and the negative sign to triplet terms. Another quantum mechanical result is that the specific mass effect is non-zero only for electron pairs with azimuthal quantum numbers l differing by one. The fractional shift in an energy level is again on the order of the electron-proton mass ratio and the isotope shift is also inversely proportional to the square of the atomic weight. The A^{-2} dependence makes mass effects small in heavy element isotope shifts ($A \geqq 140$) [6]. Experimental values of isotope shifts in the resonance lines of alkali-like spectra are compared with natural linewidth in Table 1. The increasing shift and change of sign in the heavier elements is due to volume effects to be discussed below.

Table 1. Experimental values of isotope shifts and natural widths of resonance lines of alkali-like spectra. Values are in units of mK

Element	Transition	λ [Å]	$\Delta\nu_{\text{natural}}$	$\Delta\nu_{is}$	$A_1 - A_2$
Li	$2s\,^2S_{0\frac{1}{2}} - 2p\,^2P_{\frac{1}{2},1\frac{1}{2}}$	6708	0.53[a]	337[b]	6–7
K	$4s\,^2S_{0\frac{1}{2}} - 4p\,^2P_{\frac{1}{2}}$	7699	0.20[c]	7.4[d]	39–41
Cu	$3d^{10}4s\,^2S_{0\frac{1}{2}} - 3d^{10}4p\,^2P_{\frac{1}{2}}$	3274	0.96[e]	18[f]	63–65
Rb	$5s\,^2S_{0\frac{1}{2}} - 5p\,^2P_{\frac{1}{2}}$	7948	0.19[g]	2.6[h]	85–87
Ag	$4d^{10}5s\,^2S_{0\frac{1}{2}} - 4d^{10}5p\,^2P_{\frac{1}{2}}$	3383	0.71[i]	− 15[j]	107–109

[a] M. G. Veselov, A. V. Shtoff: Opt. Spectrosc. **26**, 177 (1970).
[b] R. H. Hughes: Phys. Rev. **99**, 1837 (1955).
[c] V. I. Ostrovskii, N. P. Penkin: Opt. Spectrosc. **12**, 379 (1962).
[d] E. C. Wang, J. Yellin: Phys. Rev. A **4**, 838 (1971).
[e] M. Kock, J. Richter: Z. Astrophysik **69**, 180 (1968).
[f] P. Brix, W. Humbach: Z. Physik **128**, 506 (1950)
[g] E. L. Altman, S. A. Kanzantsev: Opt. Spectrosc. **28**, 432 (1971).
[h] H. M. Gibbs, G. C. Churchill: J. Opt. Soc. Am. **62**, 1130 (1972).
[i] P. T. Cunningham, J. K. Link: J. Opt. Soc. Am. **57**, 1000 (1967).
[j] P. Brix *et al.*: Z. Physik **130**, 88 (1951).

For heavy atoms, the dominant effect in the isotope shift is the change in nuclear charge distribution, in particular, the volume of charge in the nucleus on addition of a neutron to that nucleus. This effect is important only when the optical transition involves an s electron, since only an s electron has a non-negligible wavefunction at the nucleus. (An s electron can also cause an isotope shift even if it does not itself change energy levels. It does so through a change in its electrostatic shielding of another electron which absorbs or emits.) Inside the nucleus an s electron no longer sees a r^{-1} potential. If one assumes a uniform charge distribution inside a spherical nucleus, $\phi = (Ze/r_0)(-3/2 + 0.5\,r^2/r_0^2)$, where r_0 is the nuclear radius. The potentials for two isotopes, differing by δr_0

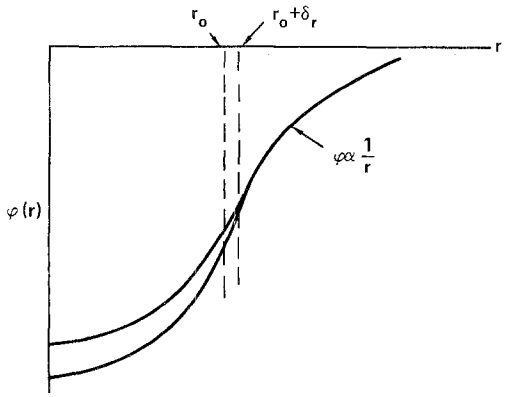

Fig. 1. The potential of two isotopes in the approximation of a spherical, uniformly charged nucleus. The heavier nucleus has the larger radius and the shallower potential well inside the nucleus. The smaller nucleus deviates less from a $1/r$ potential and binds electrons more strongly than the heavier nucleus

in nuclear radius are represented in Fig. 1. The smaller nucleus has the larger potential and the electron is more strongly bound by it since it is closer to the r^{-1} potential of a point charge. The difference in potential is given by

$$\delta\phi = -\frac{3}{2}\frac{Ze}{r_0^2}\delta r_0\left(1-\frac{r^2}{r_0^2}\right).$$

The difference in energy of an s electron in a pair of isotopes is

$$\delta w = \int_0^{r_0} \varrho_e \delta\phi dV,$$

where

$$\varrho_e = -e|\psi_s(0)|^2 \sim -\frac{e}{\pi a_0^3}\frac{Z}{n^3}$$

[7] (a_0 being the Bohr radius).

Then,

$$\delta W \sim \frac{3}{2}\frac{Z^2e^2}{\pi a_0^3 n^3}\frac{\delta r_0}{r_0}\int_0^{r_0}\left(1-\frac{r^2}{r_0^2}\right)4\pi r^2 dr$$

$$\sim \frac{r_0^2\delta r_0}{a_0^2 r_0}\frac{Z^2}{n^3}R_H \sim \frac{r_0^2}{a_0^2}\frac{Z^2}{n^3}\frac{\delta A}{A}R_H.$$

Thus the isotope shift due to the change in nuclear volume decreases inversely with atomic weight but the heavy isotope always lies higher in energy (closer to the continuum). Therefore, an electronic transition from a p orbital to a lower s orbital will be less energetic for the heavier isotope. A transition from an s orbital to a lower p orbital will be less energetic for the lighter isotope.

The assumption of a spherical nucleus which merely increases in radius when a neutron is added with $r_0 \alpha A^{1/3}$ ignores the fact the nuclei also change shape when neutrons are added. In Fig. 2 nuclear deformation, defined by the parameter $\beta^2=(a-b)^2/r_0^2$ where a and b are semimajor and semiminor axes of the nuclear ellipsoid of equivalent spherical radius r_0, is plotted against neutron number. It is apparent that only near the magic neutron numbers 50, 82, and 126 does β^2 approach zero (except for Sn which has a magic number of protons). An isotope shift results from a change in nuclear shape as well as from a change in nuclear volume. Volume effects can be accounted for in a manner similar to that discussed in the preceding paragraph but changes in shape must be accounted for, too. The potential of an ellipsoidal uniformly charged nucleus, averaged over direction, is equivalent to the potential of a charge distribution similar to Fig. 3a. The charge density is zero outside $r=a$. Inside $r=a$ it gradually increases until at $r=b$ it

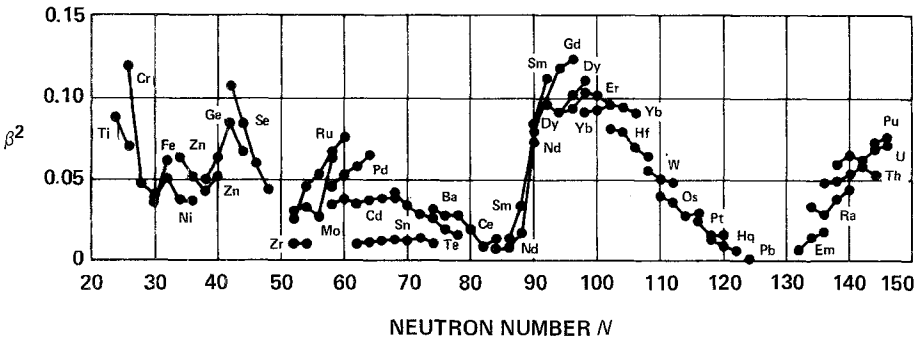

Fig. 2. The deformation of nuclei from spherical shape as a function of neutron number, N. Deformation is defined by the parameter $\beta^2=(a-b)^2/r_0^2$, where a and b are the semimajor and semiminor axes of the nuclear ellipsoid of equivalent radius r_0. Only near magic numbers does β^2 approach zero (except for Sn which has a magic number 50 of protons). The figure is taken from D. N. Stacey: Rep. Progress Phys. **29**, 171 (1966)

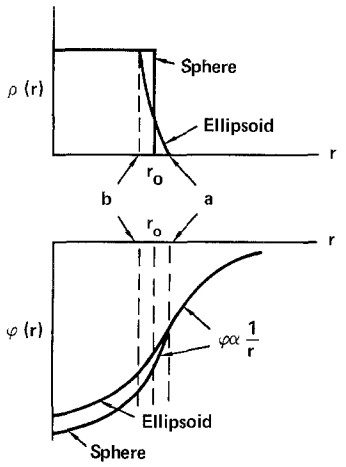

Fig. 3. (a) The charge density ϱ as a function of radius for uniformly charged elliptical nucleus, where charge has been averaged over direction, is compared to that of a sphere of equal volume. (b) The corresponding potentials are compared. It is apparent that an increase in deformation for a given nuclear volume has the same effect as an increase in nuclear volume

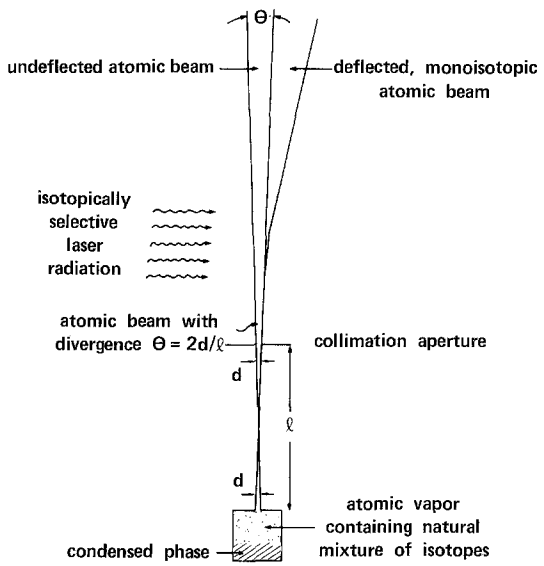

Fig. 4. Isotope separation by selective absorption of laser radiation by a single isotopic component of an atomic beam. Atomic vapor containing a mixture of isotopes effuses from a hole of diameter d. It is collimated by a similar aperture a distance l away and one isotopic component is deflected by laser radiation in the direction of its propagation

becomes $\varrho = Z/V_n$, where Z is the total nuclear charge and V_n is the volume of the nuclear ellipsoid. The potential which results from such a distribution is shown in Fig. 3b. For comparison a spherical nucleus of the same volume is shown in the figure. The potential of the ellipsoid is smaller. Thus an increase in nuclear deformation has an effect similar to an increase in volume while a decrease in nuclear deformation has the opposite effect. In certain isotope pairs, such as ^{86}Sr–^{88}Sr [8] and ^{136}Ba–^{137}Ba [9] the shift resulting from a *decrease* in nuclear deformation with the addition of one neutron is so pronounced as to cancel the shift due to the increase in nuclear volume.

The foregoing discussion is intended to give a conceptual understanding of isotope shifts in atoms. For light atoms ($A \lesssim 140$) the normal mass shift ($\Delta\nu \sim 5 \times 10^{-4} \nu/A$) is large with respect to the natural linewidth for visible transitions ($\Delta\nu \sim 2 \times 10^7$). At the upper end of this range, the two become comparable. For example, the natural linewidth in barium on the 5536 Å transition is $\Delta\nu \sim 1.9 \times 10^7$ Hz while the normal mass shift from ^{136}Ba to ^{138}Ba is 3.2×10^7 Hz [9]. On the other hand, the increase in nuclear volume, though partially cancelled by a decrease in nuclear deformation, produces a net shift (136–138) of over six times the natural linewidth on the 5536 Å transition [9, 10]. In uranium, the heaviest naturally occurring element, volume and deformation effects combine to produce typical isotope shifts in excess of 3×10^9 Hz for most lines in its extremely complex visible spectrum [11]. It is rare that various effects sum to less than the natural linewidth. Even if the isotope shifts on a given transition is small with respect to its natural linewidth, it is generally the case that another line can be found where one of the effects changes magnitude or sign with respect to the others and the resulting isotope shift becomes large.

With an excited state lifetime on the order of 10^{-8} sec, an atom can absorb and emit many times during the short interval of time it might take to transverse the laser beam. Under appropriate conditions, the number of absorption-emission events will be sufficient to physically separate the isotopic component of interest. Efficient isotope separation can be effected using an atomic beam as illustrated in Fig. 4. Atomic vapor is produced inside a container partially filled with the isotopic mixture of interest. The container is heated to bring the atomic vapor pressure of the mixture to its desired value. Atoms issue from a hole in the container and are collimated by an aperture some distance from the hole. If the gas is collisionless once it leaves the container, then the full divergence of the atomic beam above the collimation aperture is $\theta_0 = 2d/l$ in the special case where d is the width of both container and collimator apertures. The momentum of an atom

perpendicular to the atomic beam axis is $\sin\theta$ times its total momentum along the beam axis where θ is the angle between the beam axis and the atomic momentum vector. The amount of momentum which must be imparted the atom from the radiation field in order to deflect it out of the atomic beam is $Nhv/c > Mv(\sin\theta_0/2 - \sin\theta)$. Since $|\theta| < \theta_0/2$ and since θ_0 can be made very small (10^{-3} or less), the number of photons which an atom must absorb to be separated can likewise be made to be small.

The importance of the divergence of the atomic beam in the plane defined by the laser axis and atomic beam axis is two-fold. First of all, it is the largest angle through which any atom needs to be deflected in order for it to be physically removed from the original atomic beam. Secondly, it effectively determines the Doppler width of the atomic beam with respect to laser radiation incident transverse to the atomic beam axis. The shift in absorption frequency of an atom with velocity component $v\sin\theta$ in the direction of laser propagation, relative to that of an atom with zero velocity component, is

$$\Delta\nu_D = \frac{v\sin\theta}{c}\nu_0,$$

where ν_0 is the unshifted absorption frequency, and θ is the inclination of the atomic velocity vector with respect to the atomic beam axis. The distribution of atomic velocities in an atomic beam is given by

$$f(v,\theta) = 2\left(\frac{M}{2kT}\right)^2 v^3 e^{-Mv^2/2kT}\cos\theta,$$

and the distribution of velocities in a given direction perpendicular to the atomic beam axis is

$$f_\perp(v,\theta) = 2\left(\frac{M}{2kT}\right)^2 v^3 e^{-Mv^2/2kT}\cos\theta\sin\theta\cos\phi.$$

The average velocity in the beam is found from $f(v,\theta)$ to be [12]

$$\bar{v}_b = \frac{3}{4}\sqrt{\frac{2\pi kT}{M}},$$

where T is the temperature of the effusion chamber. The average velocity in the atomic beam is thus $0.75\sqrt{\pi}$ times the mean scalar velocity in the effusion chamber. The mean scalar velocity perpendicular to the atomic beam is found from $f_\perp(v,\theta)$ to be

$$v_{b\perp} = \frac{2}{3}\bar{v}_b\sin\frac{\theta_0}{2},$$

where θ_0 is the beam divergence. The Doppler width of the atomic beam is approximately the difference in absorption frequency between atoms traveling in opposite directions along the laser propagation axis with scalar velocity $\bar{v}_{b\perp}$.

$$\overline{\Delta\nu_D} = \frac{4}{3}\frac{\bar{v}_b}{c}\nu_0\sin\frac{\theta}{2}.$$

The Doppler width of the atomic beam must, first of all, be small compared to either the laser linewidth, the natural linewidth, or both. If it is not, an atom can only be deflected through a fraction of the atomic beam divergence angle and separation of a large fraction of the desired isotopic component of the atomic beam will be impossible. It is best if both Doppler and laser linewidth are small compared to the natural linewidth, although then it makes little difference whether the Doppler linewidth is greater than the laser linewidth or visa versa. The reason this arrangement is preferred is that every atom in the atomic beam sees the full laser intensity. Where the laser linewidth is greater than the natural linewidth only a fraction of the laser radiation falls within the absorption range of an atom, that fraction given approximately by $\Delta\nu_{\text{natural}}/\Delta\nu_{\text{laser}}$. The Doppler width must also be small compared to the isotope shift, otherwise several isotopic components will be deflected together.

Atomic beam divergences as small as 10^{-3} are readily achieved in practice. For example, $d = 10^{-2}$ cm and $l = 20$ cm imply such a divergence. The number of absorption-emission events required to effect separation of a given atom from an atomic beam is

$$N\frac{hv}{c} \gtrsim Mv\left(\sin\frac{\theta_0}{2} - \sin\theta\right) \sim Mv\left(\frac{\theta_0}{2} - \theta\right),$$

where the laser beam axis is perpendicular to the atomic beam axis, v is the atomic speed, and $\theta_0/2 - \theta$ is the angle between the atomic velocity vector and that defining the downwind edge of the atomic beam (the edge farthest from the laser).

Consider an "average" atom in an atomic beam with divergence $\theta_0 = 10^{-3}$. The number of photons visible laser radiation (e.g. 5500 Å) required to separate it from the original atomic beam is

$$N_0 \gtrsim M\bar{v}_b\frac{\theta_0}{2}\frac{c}{hv} \sim 9\times 10^{18}\sqrt{MkT}.$$

N_0 is largest and separation most difficult for M and T large. This is the case for a heavy atom of low volatility,

where high temperatures are required to produce appreciable vapor pressures. A refractory metal such as uranium ($A \simeq 240$) must be heated to 2450° C before its vapor pressure reaches 1 Torr. Using uranium as an example (tungsten gives almost the identical result), we have $N_0 \gtrsim 90$. This value for n_0 is a "worst case" for $\theta_0 \sim 10^{-3}$.

It remains to demonstrate that a conventional dye laser, operating with a linewidth $\lesssim 10^7$ Hz, is powerful enough to produce 10^2 successive absorption-emission events in an atom as the atom traverses the laser beam. An argon laser pumped, continuous dye laser such as those used in the experiments reported below, delivers about 50 mW of narrow linewidth tunable optical power. Operating at 5500 Å over a 1 cm^2 area this implies a flux of 1.2×10^{17} photons/cm^2 sec. The rate at which an atom will absorb is given by the photon flux times the absorption cross section. The absorption cross section at line center is given by

$$\sigma = \frac{g_2}{g_1} 4\pi \lambda\!\!\!^{-2} \quad [13],$$

where g_2 and g_1 are the degeneracies of upper and lower states, respectively

$$\frac{1}{3} \leqq \frac{g_2}{g_1} \leqq 3$$

so that for a 5500 Å transition

$$4.4 \times 10^{-10} \lesssim \sigma \lesssim 4 \times 10^{-9}.$$

Thus the absorption rate becomes

$$5 \times 10^7 \lesssim R \lesssim 4.8 \times 10^8 \text{ photons/sec}.$$

For simplicity, let $R = 10^8$. Then the average time for one absorption and one emission to take place is

$$\frac{1}{R} + \tau \simeq 2 \times 10^{-8} \text{ sec}$$

and the rate at which the absorption-emission cycle is repeated is 5×10^7/sec. Comparison of the spontaneous decay rate τ^{-1} with the absorption rate R shows that much greater laser intensities serve little purpose since they only increase the absorption rate whereas spontaneous decay is the rate limiting process [14]. One hundred absorption-emission events will take place in a time of 1.8×10^{-6} sec, or the time it takes an atom to travel a distance $\delta = 1.8 \times 10^{-6}$ v cm. For atomic vapors at 1 Torr, $\bar{v} \lesssim 3 \times 10^5$ cm/sec, so that $\delta \lesssim 0.54$ cm. The discussion which led to an absorption rate of 1.2×10^8 photons/sec assumed that the 50 mW dye laser beam was expanded to a cross section of 1 cm^2. Since $\delta \leqq 0.54$ cm, a laser beam which irradiates the atomic beam along height $h \sim 0.54$ cm parallel to the atomic beam axis is sufficient to separate an "average atom" of the desired isotope. The width can be 1.85 cm while the thickness of the atomic beam along the laser axis is determined from the divergence condition. Thus a commercial dye laser has sufficient intensity to separate isotopes on a laboratory scale and the necessary atomic beam cross section poses no practical problems with respect to laser beam expanding optics.

The principal limitation on the number of absorption-emission events per atom is the accessibility of metastable energy levels between the optically excited state and the ground state. Lifetimes of such states are many orders of magnitude longer than states whose radiative decay to the ground state is fully allowed. When an excited atom decays to such a state, it can no longer absorb laser photons and therefore cannot be further deflected. Suppose, for example, that the excited state has a probability P_1 of decaying to a metastable state and a probability P_0 of returning to the ground state. Then the probability that an atom absorbs and returns to the ground state N times before decaying to the metastable state after the $N+1^{st}$ absorption is $P_1 P_0^N$. Suppose that an "average atom" requires N_0 photons for separation. Then the fraction of atoms of the desired isotope in the beam that will be separated, is approximately

$$\varepsilon \sim P_1 \int_{n_0}^{\infty} P_0^N dN \quad \text{for large } N$$

$$= P_1 \int_{n_0}^{\infty} e^{N \ln P_0} dN = \frac{P_1}{-\ln P_0} e^{N_0 \ln P_0} \sim e^{N_0 \ln P_0}.$$

Suppose that $N_0 \sim 100$. Then $\varepsilon = 1/e$ for $N_0 \ln P_0 = -1$ and $P_1 \sim -N \ln P_0 \sim 10^{-2}$. Thus, if an average atom has to absorb (and re-emit) 100 photons in order to be separated, less than $1/e$ of the desired atoms in the beam will be separated if the probability of decay to a metastable state is more than 1%. This example, while somewhat pessimistic, illustrates the deleterious effect that even a small probability of decay into a metastable state has on the efficiency of the isotope separation. If it is not possible to avoid or tolerate metastable state accumulation, high efficiency separation can be accomplished with the use of additional lasers to excite metastable atoms to a state (e.g. the original excited state) from which they can again decay to the ground state [15]. Only when metastable states with non-negligible accumulation rates are too numerous or the

depopulating transition occurs at a frequency for which no convenient photon source exists, does efficient photodeflection become impractical.

Another limitation might be expected to arise when the density of the atomic beam in the region in which deflection takes place is too high. Induced polarization effects cause small angle atom-atom scattering. As a result of such scattering, small atomic beam divergences cannot be maintained at high beam densities. Consider the Van der Waals interaction between one atom and another passing close by it. Let v be their relative velocity and let b be the distance of closest approach in the absence of any interaction (b is called the impact parameter). If the gas is not too dense, b will generally be large enough so that the Van der Waals interaction U is weak and the angles of deflection are small. In this approximation the momentum transferred to the passing atom perpendicular to its original direction of travel is

$$P_\perp = \int_{-\infty}^{\infty} F_\perp dt = -\frac{2b}{v}\int_b^\infty \frac{dU}{dr}\frac{dr}{\sqrt{r^2-b^2}},$$

where r is the distance between the atoms [16]. The result for a $U=a/r^n$ potential is [16]

$$P_\perp = \frac{2a\sqrt{\pi}}{vb^n}\frac{\Gamma(\frac{1}{2}n+\frac{1}{2})}{\Gamma(\frac{1}{2}n)}.$$

This kind of scattering begins to have significant effect on photodeflection isotope separation when

$$P_\perp \sim N_0 \frac{h\nu}{c}$$

that is, when atoms are scattered as far as they are deflected by radiation.

The exact expression for the Van der Waals interaction is now derived [17]. The interaction of both ground and excited atoms of an isotope a with a ground state atom of a different isotope b will be considered. The unperturbed wavefunctions for the system are taken to be

$$\psi_{00}=\phi_{a0}\,\phi_{b0}, \quad \psi_{10}=\phi_{a1}\,\phi_{b0},$$
$$\psi_{01}=\phi_{a0}\,\phi_{b1}, \quad \psi_{11}=\phi_{a1}\,\phi_{b1}, \quad \text{etc.}$$

The perturbation in the Hamiltonian of alkali-like atoms is given by

$$V=-\frac{e^2}{r_{Ba}}-\frac{e^2}{r_{Ab}}+\frac{e^2}{r_{AB}}+\frac{e^2}{r_{ab}},$$

where r_{Ba} is the distance between the nucleus of isotope b and the electron of isotope a, r_{Ab} is the distance between the nucleus of isotope a and the electron of isotope b, and so on. The perturbation Hamiltonian can be expanded into dipole-dipole interaction, dipole-quadrupole interaction, quadrupole-quadrupole interaction, etc. Keeping only the dipole-dipole part, the perturbation becomes

$$V_d = \frac{e^2}{R^3}(x_a x_b + y_a y_b - 2z_a z_b),$$

where $R=r_{AB}$ and x_a, x_b, z_a are the coordinates of the electron. The first order perturbation in the energy is zero

$$E_1 = \langle\psi_{ij}|V_d|\psi_{ij}\rangle = 0.$$

The second order perturbation in the energy is

$$E_2 = \sum_{k,l}\frac{\langle\psi_{ij}|V_d|\psi_{kl}\rangle\langle\psi_{kl}|V_d|\psi_{ij}\rangle}{E_{ij}-E_{kl}}.$$

Thus, for example, the energy of interaction of ground state atoms is

$$E_2 = \frac{\langle\psi_{00}|V_d|\psi_{11}\rangle\langle\psi_{11}|V_d|\psi_{00}\rangle}{2h\nu_{10}} + \ldots.$$

This leads to the expression for the Van der Waals interaction given by London [17]

$$U = -\frac{3}{4}\frac{\alpha^2}{r^6}I,$$

where α is the atomic polarizability, I is the ionization potential and r is the distance between the interacting atoms. For one isotope excited and one in the ground state we have

$$E_2 = \frac{\langle\psi_{10}|V_d|\psi_{01}\rangle\langle\psi_{01}|V_d|\psi_{10}\rangle}{\hbar\delta\nu} + \ldots,$$

where now the denominator is $\hbar$ times the isotope shift. Thus, because the energy of the system in which isotope a is excited while isotope b is in the ground state, is almost identical to the system in which isotope b is excited and isotope a is in the ground state, the perturbation is larger by about a factor of $2\nu/\delta\nu$.

The expression for transverse momentum imparted by the scattering process now becomes

$$P_\perp \sim \frac{4\sqrt{\pi}}{3}\frac{e^4\bar{r}_a^2\bar{r}_b^2}{vb^6h\delta\nu}\frac{\Gamma(\frac{7}{2})}{\Gamma(3)},$$

where $\bar{r}_a = |\langle\phi_{a0}|r_a|\phi_{a1}\rangle|^2$ or

$$P_\perp \sim \frac{3}{2}\sqrt{\pi}\frac{\alpha^2 I}{vb^6}\frac{\Gamma(\frac{7}{2})}{\Gamma(3)}\frac{2\nu}{\delta\nu}.$$

For most atoms $10^5 \lesssim 2\nu/\delta\nu \lesssim 10^8$ so that the increase in scattering angle resulting from excitation of one isotopic species is impressive. The relation $P_\perp \sim N_0 h\nu/c$ defines a total cross section for the scattering process, namely

$$\sigma_s \sim \pi b^2 \sim \pi \left(N_0 \frac{h\nu}{I} \frac{v}{c} \frac{\delta\nu}{\nu} \frac{1}{5\sqrt{\pi}\,\alpha^2} \right)^{-1/3} \text{cm}^2 .$$

With $\frac{h\nu}{I} \sim \frac{1}{5}, \frac{v}{c} \sim 10^{-6}, \frac{\delta\nu}{\nu} \sim 10^{-7}$ and $\alpha \sim 3 \times 10^{-23}$ cm, the above condition becomes

$$\sigma_s \sim 2 \times 10^{-10} (N_0)^{-1/3} \text{ cm}^2 .$$

The number density in the gas must be such that $\frac{1}{n\sigma_s} \gg N_0 \tau v$ where $N_0\tau$ is the time an atom spends in the excited state before it is separated. Thus $n \ll 2 \times 10^{13} (N_0)^{-2/3}$ atom/cm^3. It is assumed that N_0 is small enough that metastable accumulation does not significantly limit the separation process.

The density of atoms at the source of the atomic beam is given by the relation

$$n = \left(\frac{r_0}{r} \right)^2 \frac{n_0}{6},$$

where n is the density of atoms a distance r from the source aperture whose radius is r_0. Thus, the source density is governed by the inequality

$$n_0 < 6 \left(\frac{r}{r_0} \right)^2 n_{\max} = \frac{6 n_{\max}}{\left(\frac{\theta_0}{2} \right)^2},$$

where θ_0 is the divergence of an atomic beam defined by identical source and collimater holes of radius r_0. With $\theta_0 \sim 10^{-2}$ and $n_{\max} \sim 2 \times 10^{13} (N_0)^{-2/3}$ the source density cannot exceed $4 \times 10^{18} (N_0)^{-2/3}$ atoms/cm^3.

Another process which one might expect to limit efficiency and produce fractional enrichment is excitation exchange between different isotopes. The density at which excitation exchange becomes likely is given approximately by

$$\frac{E_2}{h\delta\nu} \sim 1 ,$$

where E_2 is the second order perturbation of the energy of a system containing one excited atom of isotope a and one ground state atom of isotope b and $\delta\nu$ is the isotope shift on the corresponding transition. Thus excitation exchange is likely for distances R less than that given by

$$\frac{e^4}{R^6} \frac{|r_{01}|^4}{(h\delta\nu)^2} \sim \frac{3}{2} \frac{\alpha^2}{R^6} \frac{I}{h\nu} \left(\frac{\nu}{\delta\nu} \right)^2 \sim 1 .$$

The total cross section is given by

$$\sigma_e = \pi R^2 \sim \pi \left[\frac{2}{3\alpha^2} \frac{h\nu}{I} \left(\frac{\delta\nu}{\nu} \right)^2 \right]^{1/3} .$$

Using the same numbers as were used in the scattering example, the cross section for excitation exchange becomes $\sigma_e \sim 10^{-9}$ cm^2. Since photodeflection relies on momentum transfer from many absorption emission events, however, excitation transfer has little effect. Excitation exchange is equivalent to emission by an atom of the desired isotope and absorption by an adjacent atom. It therefore does not affect the deflection of the desired isotope which depends on absorption alone. An atom of the unwanted isotope can gain momentum in the process, but the direction of momentum change is random. Furthermore, a single unit of momentum $h\nu/c$ is far from sufficient to produce separation. If N units of momentum are required to deflect an average atom out of the beam, then, because of the isotropic nature of the excitation transfer process, an atom of unwanted isotope would have to take part in an average of N^2 excitation transfers to be separated. Thus only very small contamination could result even if the density of the atomic beam were high enough to make excitation transfer a significant process. Only in a separation process which relies on energy transfer from the radiation field [18–20] does excitation exchange pose a significant limitation on atom density.

2. Barium Isotope Separation

Barium is element number 56 on the periodic table of the elements. It has seven stable isotopes which are listed in Table 2 along with their natural abundances. The heaviest isotope, ^{138}Ba, is also the most abundant. In heavier elements of even Z, isotopic abundances are

Table 2. Natural abundance of barium isotopes

Isotope	% Natural Abundance
130	0.10
132	0.10
134	2.42
135	6.59
136	7.81
137	11.32
138	71.66

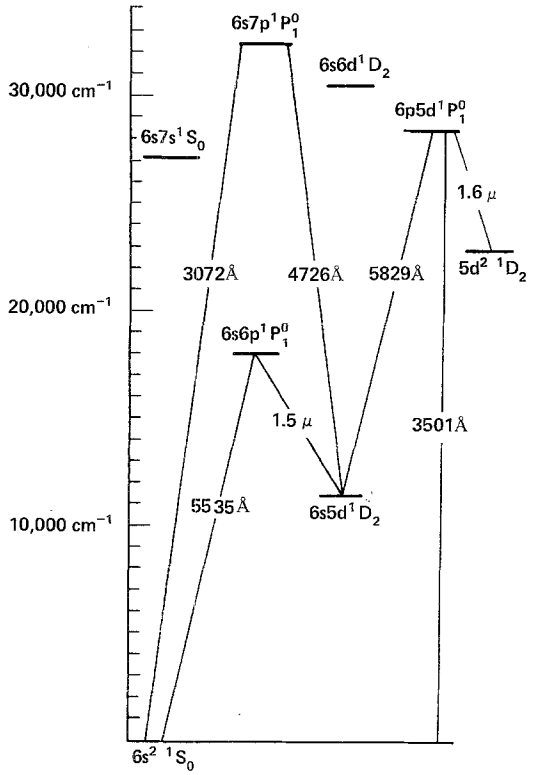

Fig. 5. Low lying singlet energy levels and selected transitions in Ba I

usually largest for moderately heavy isotopes, smaller for the heaviest isotope and smallest for the lightest isotope. The unusual ^{138}Ba abundance is a result of the face that ^{138}Ba has 82 neutrons, one of the magic numbers of nuclear structure, analogous to noble gas electronic structure, and very stable.

Barium is an alkali earth element, in its ground state barium has two 6s electrons outside of a closed shell xenon electronic structure. An energy level diagram of low lying singlet states is given for reference in Fig. 5. The barium resonance line, $6s^2\ ^1S_0$–$6s6p\ ^1P_1$, occurs at a wavelength of 5535.7 Å. This transition gives a flame containing barium its characteristic green color. Since a number of dyes lase efficiently at 5535.7 Å, the barium resonance could be used to demonstrate photodeflection isotope separation.

Barium is a metallic solid at room temperature. It melts at 725° C and boils at 1638° C. The liquid has a vapor pressure of 1 Torr at 800° C. An atomic beam effusing from an 800° C source would have an average velocity of

$$\bar{v}_b = \frac{3}{4}\sqrt{\frac{2kT}{M}} \sim 6\times 10^4 \text{ cm/sec},$$

which implies that the number of absorption-emission events required to separate an "average" atom from an atomic beam of divergence θ_0 is

$$N_0 \sim M\bar{v}_b \frac{\theta_0}{2}\frac{c}{h\nu} \sim 4\times 10^4\,\theta_0 .$$

The lifetime of the upper $6s6p\ ^1P_1$ state is 8.37×10^{-9} sec [21, 22] which implies a 19 MHz natural linewidth. It has been noted that both laser and Doppler linewidth should be small compared with the natural linewidth. This is not difficult, since laser linewidths of as little as 10^5 Hz can be achieved [23, 24], while a Doppler width small compared to 19 MHz implies

$$\Delta\nu_D \sim \frac{4}{3}\frac{\bar{v}_b}{c}\sin\frac{\theta_0}{2}\nu_0 \sim 8\times 10^8\,\theta_0 \ll 1.9\times 10^7$$

or

$$\theta_0 \ll 2.4\times 10^{-2} \text{ rad}.$$

In barium, a single metastable state is accessible from the $6s6p\ ^1P_1$ level. This is the $6s5d\ ^1D_2$ state from which decay to the ground state is parity forbidden, being allowed only via an electric quadrupole transition. The $^1D_2$ state thus has a lifetime given approximately by $\tau^{-1} \sim 0.5$ sec [25]. An excited barium atom in the atomic beam which decays to the $^1D_2$ state will not return to the ground state to undergo further deflection before it has, on the average, traveled ~ 300 m.

The probability that an excited atom decays into the metastable state once excited, relative to the probability that it decays to the ground state, is found from the ratio of spontaneous decay rates for the two transitions. Recalling the expression for the decay rate to a single state,

$$\tau_{12}^{-1} = \frac{8\pi e^2}{mc}\frac{f_{12}}{\lambda_{12}^2}\frac{g_2}{g_1},$$

the ratio of spontaneous decay rates for the $6s6p\ ^1P_1$ level in barium is found, using published values of the oscillator strengths, [26] to be

$$\frac{g_s}{g_d}\frac{f_s}{f_D}\frac{(\lambda_D)^2}{(\lambda_s)^2} = \frac{1}{5}\frac{1.59}{0.10}\frac{(15000)^2}{(5535)^2} \simeq 24 .$$

Thus, for a given atom in the ^1P state, the probability that it radiates into the ^1D state is 1/25. The probability that a given atom scatters N photons before being pumped into the metastable level is $(24/25)^N/25 = e^{-0.04N}/25$ and the separation efficiency is approximately

$$\varepsilon \sim e^{-0.04\times 4\times 10^4\theta_0} \sim e^{-1.6\times 10^3\theta_0} .$$

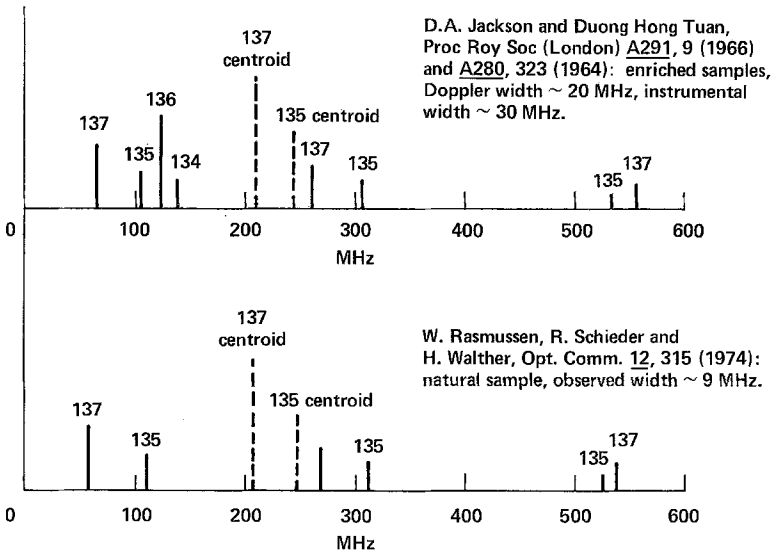

Fig. 6. Isotopic-hyperfine structure of the 5536 Å Ba resonance

The actual efficiency was found to be much greater than this expression implies. The error in the "average atom" approximation is not large. Rather, the 6s6p $^1P_1$–6s5d $^1D_2$ oscillator strength was found to be high so that decay to the metastable state from the 6s6p $^1P_1$ level was less probable than expected [15].

Barium isotopes exhibit unusually small isotope shifts. The positions of isotopic absorption peaks on the 5536 Å transition reported by recent investigators are summarized in Fig. 6. The absorption spectrum of natural barium has nine components (excluding the rare ^{130}Ba and ^{132}Ba isotopes): one component for each of the even isotopes 134, 136, and 138, and three for each of the odd isotopes 135 and 137 (nuclear spin 3/2). From Fig. 6 it would appear that most, if not all, isotopic absorptions of barium are spaced by more than the natural linewidth of 19 MHz for the 5535.7 Å transition. In as much as isotope shifts in barium are among the smallest measured, barium was regarded as an unusually challenging test of the photodeflection method of isotope separation.

3. Experiment

A diagram of the experimental set-up is given in Fig. 7. The 5536 Å laser radiation is produced by a Spectra

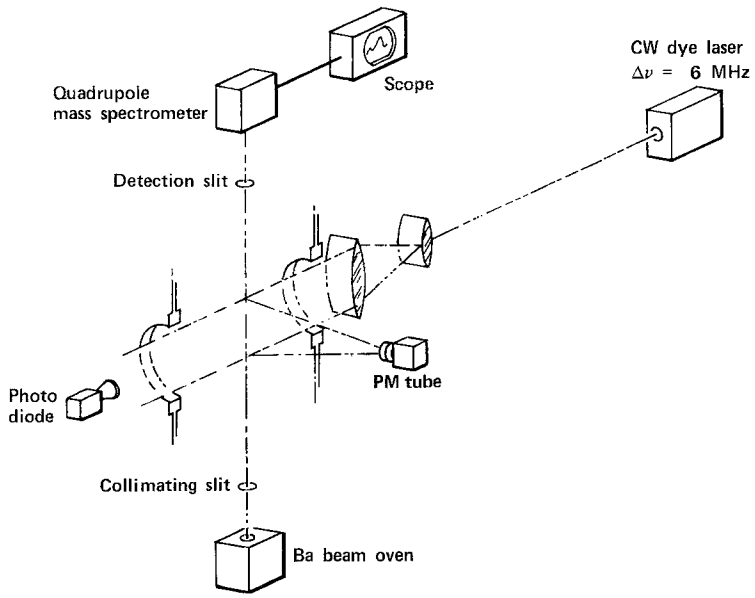

Fig. 7. The experimental arrangement used for Ba isotope separation

Physics model 370/581 dye laser [27] which employs a 2×10^{-4} M solution of Rh6G in a 3:1 mixture of water and hexafluoro-2-propanol. It is pumped by a 1.6 W (all line) Argon laser and gives 40 mW of output power in a 6×10^{-5} Å (6 MHz) wide band [28]. Long term drift was less than 5 MHz over tens of minutes [28].

The barium is evaporated inside the vacuum system with residual pressure $\sim 10^{-7}$ Torr. The barium is held inside a double crucible. The inner crucible is ~ 12 mm in outer diameter and is 12 mm high. It is made of 1.6 mm thick molybdenum with a sharp upper edge to prevent liquid barium from migrating over the wall and into the outer crucible (and out of the outer crucible in the same way). The outer crucible has an outer diameter of 19 mm. It is 19 mm high and 3.1 mm thick. A molybdenum top was machined to fit tightly over the outer crucible. The top has a 0.05 cm diameter hole in it from which barium vapor can effuse.

The crucibles are radiatively heated from a surrounding resistively heated molybdenum jacket. Temperature is monitored using a Pt–Rh thermocouple located inside the pedestal which supports the crucibles. The heating element is surrounded by five 0.025 mm thick tungsten foil radiation shields to prevent excessive heat loss.

Twelve centimeters above the crucible there is a slot 0.05 cm wide and 0.2 cm long, defined by two razor blades, which collimates the effusive atomic vapor. The divergence of the resulting atomic beam across its narrow dimension is ~ 8 mrad. At a source density of 2×10^{16} atoms/cc, approximately 10^{13} atoms/sec (0.2 mgm/day) pass through this aperture into the deflection region.

No effort was made to maximize throughput, although only about 1% of the dye laser power was scattered in the process of separating the abundant ^{138}Ba isotope (and much less for other isotopes). Scaling of the barium system is, of course, rather simple in principle. For example, 5 cm wide effusion slots (instead of holes) could be stacked 100 deep. Then 100 dye laser beams side by side could be used to separate roughly 10^{17} atoms/sec (or 2 gm/day). The scaling problem was considered to be quite secondary to the problem demonstrating the method and defining its limitations. It should be noted, however, that the photodeflection method employs bound state transitions which have very large absorption cross sections and, as such, does not require high power lasers. In particular, comparatively low power continuous wave lasers can be employed in photodeflection schemes, while other methods which involve ionization or dissociation require lasers more than 10^7 times more powerful. Scaling and efficiency considerations then involve problems of *average* laser power as well as simple unit replication.

Just above the collimater the green laser beam intersects the atomic beam at a right angle (alignment procedures permitted definition of a right angle to better than one part in fifty). The green laser beam, initially 3 mm in diameter, is expanded through a cylindrical telescope by a factor of 10. The reason for expanding the beam is that the 5536 Å barium resonance is saturated at an intensity of about 100 mW/cm^2. At this intensity the absorption rate is approximately equal to the spontaneous emission rate. In the same manner as that discussed earlier, higher intensities increase the absorption and stimulated emission rates but not the total momentum transfer rate which is limited by the spontaneous emission rate at intensities above the saturation intensity. Furthermore, the excess photon flux is not scattered whereas in an expanded beam, whose intensity is below the saturation intensity, those same photons can be scattered by the atomic beam and produce a corresponding deflection.

Radiation scattered by the atomic beam is monitored by a photomultiplier tube (RCA 931A) [27]. Light enters the photomultiplier via a long straight tube which excludes stray radiation.

Twenty centimeters above the collimating aperture, a second aperture is placed in the path of the atomic beam. Its purpose is to pass either the separated or the unseparated portion of the atomic beam, while blocking the other portion. The aperture is defined by two razor blades separated by 0.4 cm. They are mounted on a platform which can be translated back and forth on the deflection (laser) axis from outside the vacuum chamber by use of a rotary motion feed-through driving a worm gear.

Directly above the second aperture is the ionizer of the EAI Model 200 quadrupole mass spectrometer [27]. The axis of the quadrupole is perpendicular to the atomic beam. The spectrometer head is mounted in such a manner that it can be moved slightly, permitting its signal to be maximized by optimizing the position of the atomic beam within the ionizer.

4. Results

4.1. Fluorescence Spectrum of Natural Barium on the $6s^2\ ^1S_0$–$6s6p\ ^1P_1$ 5536 Å *Transition*

To observe the fluorescence spectrum of natural barium on the 5536 Å transition, the dye laser frequency was

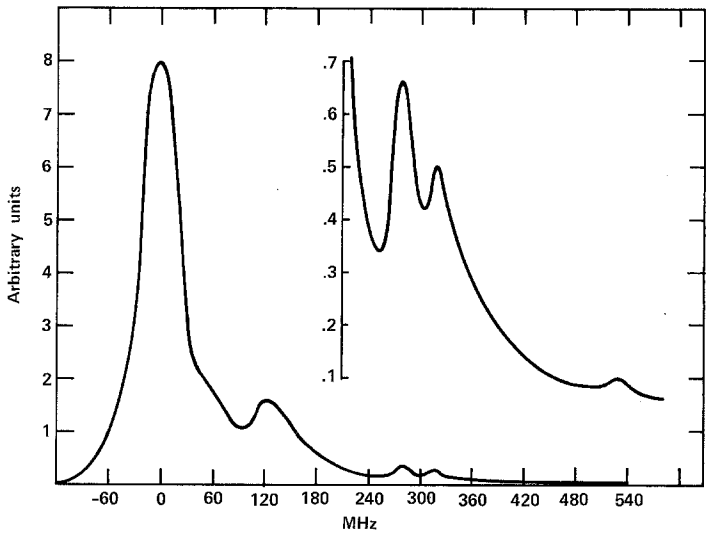

Fig. 8. Observed fluorescence spectrum of Ba I on the 5536 Å resonance

swept linearly through the atomic resonance using the piezoelectrically driven cavity mirror mount and etalon spacer. The intensity of radiation scattered from the atomic beam was monitored by the photomultiplier tube and displayed on an oscilloscope. The resulting fluorescence curve is given in Fig. 8. Six peaks are observed. The largest peak must be assigned to the abundant (72%) ^{138}Ba isotope, and the relative positions of the other peaks are referred to the center of this peak. Other fluorescence peaks are observed at about 60, 130, 280, 320, and 530 MHz. Since there are a total of nine components in the spectrum of the abundant barium isotopes, certain observed peaks must contain more than one component. Isotopic determination can be made using enriched samples, which are very expensive since such samples are available only from electromagnetic separation processes (i.e. Calutron). However, the experimental arrangement described in the preceding section (Fig. 7) permitted mass analysis of the separated atoms and hence assignment of isotopic composition to each absorption peak [15].

4.2. Observation of Metastable State Accumulation

The intensity of the laser beam after passing through the cylindrical telescope was about 50 mW/cm^2. It illuminated the atomic beam along a 3 cm path (see Fig. 7). When the laser frequency was swept through the ^{138}Ba resonance the following process occurred. As the laser frequency increased approaching the ^{138}Ba resonance line center, the scattered light from all parts of the illuminated atomic beam increased in intensity. When laser frequency got within about 10 MHz of exact resonance, however, the upper part of the illuminated atomic beam began to dim while the lower part continued to become brighter. At exact resonance only the lower $\sim 1/3$ of the illuminated atomic beam continued to scatter brightly while the rest fluoresced only quite dimly. As the laser frequency continued past the ^{138}Ba resonance the process just described happened in reverse.

The explanation for the dimming of the upper part of the illuminated atomic beam is that most ^{138}Ba atoms have fallen into the 6s5d $^1D_2$ state in the first centimeter of the illumination region and can no longer scatter 5536 Å radiation. This effect is not due to Doppler shift as a result of deflection, because when a second laser operating at 5826 Å is used to depopulate the metastable state via excitation to the 5d6p $^1P_1$ state, the upper portion of the atomic beam no longer diminishes in 5536 Å fluorescent intensity.

An experiment was undertaken to quantify the metastable state accumulation process. The original experimental set-up was changed as illustrated in Fig. 9. The mass spectrometer was removed from its port on the vacuum chamber and the slit just below the ionizer was removed as well. A window was put on the vacant port. The green laser beam was split before entering the cylindrical telescope so that about 5% of the original beam intensity could be directed through the new window to illuminate the atomic beam at a point about 20 cm above the collimation slit. The atomic and probe laser beams again intersected at right angles. Another photomultiplier tube with a 10 cm snout was aimed at

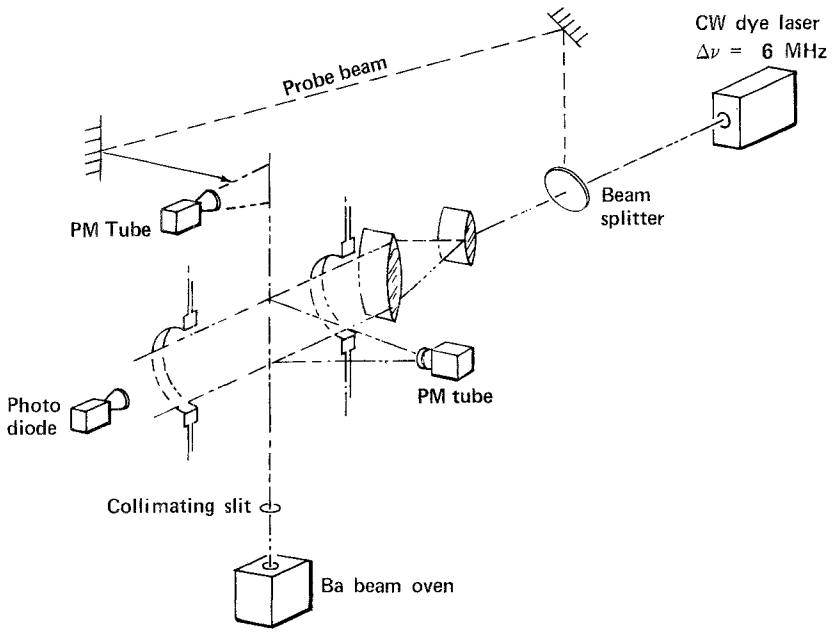

Fig. 9. Experimental arrangement used to observe metastable state accumulation

the new intersection to detect 5536 Å fluorescence from this part of the beam.

Figure 10a is a trace of this fluorescence intensity vs. frequency with the main laser blocked off at the telescope. It is, of course, identical to Fig. 8. Figure 10b is again a trace of scattered intensity vs. frequency but the main laser beam is no longer blocked and the metastable accumulation process occurs in the lower interaction region. This causes a dip in scattered probe laser beam intensity exactly at the ^{138}Ba absorption center. The amplitude at the dip is 2.5 mV while the amplitude of the peak in Fig. 10a is 85 mV. Thus only about 3% of the ^{138}Ba enters the probe laser beam in the ground state. The rest must be in the 6s5d $^1D_2$ metastable state. It is apparent, therefore, that metastable state accumulation will limit the efficiency and extent of isotope separation without some means of metastable state depopulation.

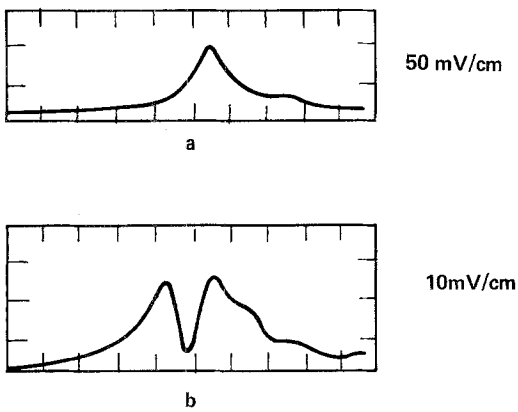

Fig. 10a and b. Scattered fluorescence intensity from the probe laser beam as a function of intensity with (a) main laser beam blocked and (b) main laser beam on metastable state accumulation is most pronounced at the center of the isotopic 5536 Å absorption peak as expected

4.3. Isotope Separation

Isotope separation without metastable state depopulation has been observed in the experimental arrangement of Fig. 7. The electron energy in the mass spectrometer ionizer was set at 10 eV. Such a low energy had the advantage of eliminating hydrocarbon background. It is clear from the previous section that most deflected atoms will enter the ionizer in the 6s5d metastable state. At 10 eV electron energy, the ionizer was found to be about twice as efficient in generating ions from metastable atoms than from ground state atoms (see below). This further increased the signal to noise ratio. The mass spectrometer output was filtered to eliminate rf pickup, amplified using a Tektronix 1A7 plug-in, and averaged by means of a Princeton Applied Research TDH9 Waveform Eductor [27]. In this manner, barium atom densities as low as 3×10^4/cc could be reliably detected. A quadrupole unit of more recent design could improve this figure.

Figure 11a shows the mass spectrometer output when only the deflected portion of the atomic beam was allowed to enter the ionizer of the mass analyzer. The

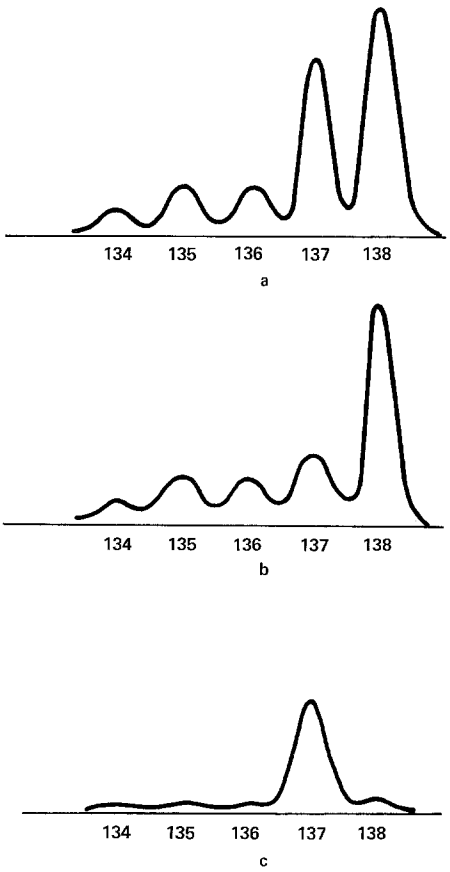

Fig. 11a—c. Mass analysis of deflected portion of the atomic beam: (a) laser frequency 280 MHz above the 138 Ba resonance; (b) laser off – the signal results from background barium; (c) deflected barium mass analysis compensated for background barium

laser frequency was 280 MHz greater than the ^{138}Ba resonance. Figure 11b shows the output with laser beam blocked. It is seen that the ^{137}Ba signal in Fig. 11a is greatly enhanced over the background signal in Fig. 11b. It should be noted that the barium outside the atomic beam defined by crucible hole and collimation slit, comes from atoms which issued the crucible in a direction which prohibited its direct escape through the hole in the oven's heat shielding. These atoms must make several collisions with surfaces or other atoms before escaping. The resulting "background beam" is defined by the hole in the heat shielding and the collimating slit. A more sophisticated oven design could eliminate the background beam.

If one subtracts amplitudes of Fig. 11b from those of Fig. 11a one obtains Fig. 11c. Since all peaks in Fig. 11c except for ^{137}Ba are the result of subtracting two large numbers, the relative error is large. It is safe to say,

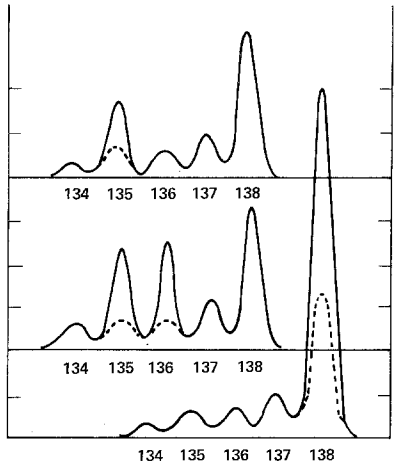

Fig. 12a—c. Mass analysis of deflected portion of the atomic beam with laser frequency (a) 310 MHz, (b) 130 MHz, and (c) 0 MHz above the ^{138}Ba resonance. The dotted line indicates the signal when the laser is blocked

however, that the purity of ^{137}Ba in the deflected beam is greater than 90% since uncertainty in the height of the peaks is $<5\%$. It should be noted that the absence of any noticable change in the ^{138}Ba peak implies that Van der Waals scattering is not significant at these beam densities and isotope shifts. If it were, one would expect Fig. 11c to show equal peaks heights for masses 138 and 137.

Figure 12a–c are analogous to Fig. 11a. Figure 12a shows separation of ^{135}Ba at 322 MHz. Again, the purity of the ^{135}Ba is $\gtrsim 90\%$. This represents more than a 13 fold enrichment.

Figure 12b displays the mass analyzer signal with the laser frequency 128 MHz above the ^{138}Ba resonance. Here several isotopes are separated at once. This is the result of the proximity of three isotopic-hyperfine absorption peaks: ^{135}Ba at 120 MHz, ^{136}Ba at 128 MHz, and ^{134}Ba at 138 MHz. These three absorptions appear as a single peak in the absorption spectrum of Fig. 8.

Figure 12c shows separation of ^{138}Ba. Visual observation of the atomic beam revealed the deflection of the ^{138}Ba clearly. The fact that the beam "tilted" rather than "spread" symmetrically implies that the density of the atomic beam was also insufficient to favor scattering processes involving resonant interaction of excited ^{138}Ba atoms with ground state ^{138}Ba atoms [17]. Resonant interactions have non-zero first order terms in the electrostatic perturbation. Thus they fall off as R^{-3} instead of R^{-6} and are larger than the near-resonant Van der Waals interactions.

The data of Figs. 11 and 12 show that isotope separation has been achieved in the experimental arrangement described. It also demonstrates the potential which the method possesses for producing isotopically pure product. Only when optical overlap occurs is there significant isotopic mixing in the deflected beam. It has been noted several times that the isotope shifts in barium are anomalously small. Even here complete isolation of each isotope is possible on at least one line with the exception of ^{136}Ba and ^{134}Ba. To obtain a high purity sample of ^{136}Ba it would be necessary to perform the separation in at least 2 steps: (a) separation of ^{136}Ba with significant impurities of ^{134}Ba and ^{135}Ba at $\Delta\nu = 128$ MHz, (b) elimination of the ^{135}Ba impurity by deflection at $\Delta\nu = 322$ MHz. This now leaves ^{136}Ba with a ^{134}Ba impurity. Increased purity requires one or more separation steps at 128 MHz. Hence, in spite of anomalously small isotope shifts, separation of each isotope of barium is possible with the laser deflection technique.

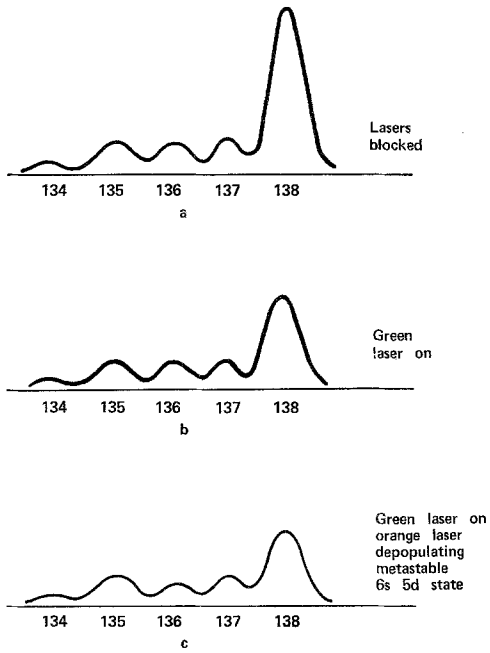

Fig. 13a—c. Mass analysis of the depleted atomic beam (the deflected portion is blocked): (a) laser blocked, (b) 5536 Å laser on, (c) 5536 Å laser on with a second laser at 5836 Å depopulating the 6s5d $^1D_2$ level to obviate the increased sensitivity of the mass analyser to metastable atoms

4.4. Separation Efficiency

It has been seen that isotopically pure samples of barium can be obtained using photodeflection isotope separation. It remains to determine with what efficiency isotopes can be separated by this model, i.e. what fraction of the desired isotope present in the original beam, can be removed from it.

The experimental arrangement was the same as that of the previous section except that now the slit below the ionizer was adjusted to pass only the original beam. Any atom which was deflected through an angle large enough to emerge from the original beam could not pass through the aperture.

Figure 13a shows the mass analyzer output with the laser blocked. Figure 13b exhibits the same output with the laser on at the absorption frequency of ^{138}Ba. The ^{138}Ba signal with the laser on is only 60% of what it is with the laser blocked indicating, it would seem, that 40% of the ^{138}Ba in the atomic beam is being separated when the laser is on. However, since nearly all the atoms which enter the ionizer are in the metastable state, the signal of Fig. 13b is spuriously high.

It has been mentioned previously that the ionizer is at least twice as efficient in this case. This result is obtained by comparison of Fig. 13b with Fig. 13c. In the latter, the second dye laser, operating on the ^{138}Ba 6s5d $^1D_2$–6p5d $^1P_1$ transition of 5826 Å, was used to depopulate the metastable atoms after they passed through the green beam. The green and orange beams were not allowed to overlap, thus avoiding the possibility that an atom, having been returned to the ground state via the 6p5d level, would then be further deflected by absorption and emission on the 5536 Å transition. A single pass of the orange laser was sufficient to *completely* depopulate the metastable state. This is demonstrated by the fact that only in the lower 1/3 or less of the region in which the orange laser beam and the atomic beam intersect, does the 5826 Å radiation scatter strongly. The upper 2/3 or more was very dim indicating absence of 6s5d atoms. In addition, when the 5826 Å beam was reflected back onto the atomic beam, just above its position on the initial pass, no change in the mass spectrometer output was observed although the first pass dropped its output, as shown in Fig. 13c by a factor of 0.7. This would seem to indicate an ionizer efficiency which is a little over 40% greater for 6s5d atoms than for ground state atoms but decay from the 6p5d state into the metastable $5d^2$ state has not yet been accounted for. Clearly, if a significant fraction of 6s5d metastable atoms end up in the $5d^2$ metastable state, then the amplitude of Fig. 13c is still spuriously high. It has been determined [15] that the rate of decay into the $5d^2$ metastable state is 2/3 the rate of decay to the ground state. Thus, 60% of

the metastable atoms will end up in the ground state while 40% will end up in the $5d^2$ metastable state. Figure 13c has 70% the peak height of Fig. 13b. If it is assumed that the ionization rate from the 6s5d state is the same as that from the $5d^2$ state, then the peak amplitude with complete depopulation will be 1/2 that of Fig. 13b:

Let $A_{6s5d}C=1$ be the signal observed with C atoms/cc in the 6s5d state. Similarly, let $A_{6s^2}C$ be the signal with C atoms/cc in the $6s^2$ state. Knowing the decay probabilities from the 6p5d state and the observed signal we can write

$$0.6\,A_{6s^2}C+0.4\,A_{5d}C=0.7$$
$$0.6\,A_{6s^2}C+0.4=0.7$$
$$A_{6s^2}C=0.3/0.6=0.5\,.$$

The assumption that the ionization rate from the $5d^2$ state is the same as that from the $6s5d^2$ is conservative. Certainly the presence of the second 5d electron in the $5d^2$ metastable state will increase the ionization rate relative to that from the 6s5d state and may result in greater ionizer efficiency if the latter is not already close to unity.

The corrected ^{138}Ba signal with the green laser is then less than 30% of the ^{138}Ba signal with the laser off. This indicates that at least 70% of the ^{138}Ba is actually being separated without metastable state depopulation. The efficiency, of course, depends on the metastable state accumulation rate and on the divergence of the atomic beam. The figure of 70% for the efficiency can be improved either by using a second laser to depopulate the metastable state or by using a smaller divergence atomic beam or both.

Acknowledgements. The author wishes to thank Dr. Lowell Wood and Professor Edward Teller for their support and active interest. He also acknowledges the skilled assistance of Mr. D. E. Duerre and Mr. J. R. Simpson in the experimental work presented here.

References

1. A. Ashkin: Phys. Rev. Letters **25**, 1321 (1970)
2. A. F. Bernhardt, D. E. Duerre, J. R. Simpson, L. L. Wood: Appl. Phys. Letters **25**, 617 (1974)
3. H. Figger, H. Walther: Z. Physik **267**, 1 (1974)
4. H. Kopfermann: *Nuclear Moments* (Academic Press, New York 1958), pp. 161—167
5. D. J. Hughes, C. Eckart: Phys. Rev. **36**, 694 (1930)
6. H. Kopferman: *Nuclear Moments* (Academic Press, New York 1958), p. 167
7. H. Kopferman: *Nuclear Moments* (Academic Press, New York 1958), p. 124
8. R. D. Ehrlich, D. Fryberger, D. A. Jensen, C. Nissim-Sabat, R. J. Powers, V. L. Telegdi, C. K. Hargrove: Phys. Rev. Letters **18**, 959 (1967)
9. D. A. Jackson, Duong Hong Tuan: Proc. Roy. Soc. (London) A**291**, 9 (1966)
10. This work
11. D. W. Steinhaus, M. V. Phillips, J. B. Moody, L. J. Radziemski, Jr., K. J. Fisher, D. R. Hahn: "The Emission Spectrum of Uranium between 19080 and 30261 cm^{-1}", Los Alamos Scientific Laboratory, Report LA-4944 (1972)
12. N. Ramsey: *Molecular Beams* (Oxford Press, Oxford 1956), p. 21
13. J. D. Jackson: *Classical Electrodynamics* (John Wiley & Sons, New York 1962), p. 605
14. This is true when emission is spontaneous. Stimulated emission can be used to produce deflection, too. Such schemes have been proposed by A. Szoke and I. Nebenzahl, Appl. Phys. Letters **25**, 327 (1974) and A. F. Bernhardt, D. E. Duerre, J. R. Simpson, J. Goldsborough, C. Jones: VIII Intern. Conf. on Quantum Electronics, San Francisco, Calif. (1974), Paper Q-12
15. A. F. Bernhardt, D. E. Duerre, J. R. Simpson, L. L. Wood: To be published
16. L. D. Landau, E. M. Lifschitz: *Mechanics* (Pergamon Press, New York 1960), Chapter IV
17. F. London: Z. Phys. **63**, 245 (1930). For a general treatise see H. Margeneu and N. R. Kestner, *Theory of Intermolecular Forces.* (Pergamon Press, New York 1969)
18. R. V. Ambartzumian, V. S. Letokhov: Appl. Opt. **11**, 354 (1972)
19. U. Brinkman, W. Hartig, H. Telle, H. Walther: Appl. Phys. **5**, 109 (1974)
20. S. A. Tuccio, J. W. Dubrin, O. G. Peterson, B. B. Snavely: "Two Step Selective Photoionization of ^{235}U in Uranium Vapor", VIII Intern. Quantum Electronics Conf., San Francisco, Calif. (June 1974), Paper Q-14
21. L. O. Dickie, F. M. Kelly: Can. J. Phys. **48**, 879 (1970)
22. M. W. Swagel, A. Lurio: Phys. Rev. **169**, 114 (1968)
23. R. L. Barger, M. S. Sorem, J. L. Hall: Appl. Phys. Letters **22**, 573 (1973)
24. F. Y. Wu, R. E. Grove, S. Ezekiel: Appl. Phys. Letters **25**, 73 (1974)
25. P. McCavert, E. Trefftz: J. Phys. B**7**, 1270 (1974)
26. B. M. Miles, W. L. Wiese: U. S. Natl. Bur. Stand. Tech. Note 474
27. The research equipment and materials designated by brand name in this paper are for identification purposes only, and do not imply the endorsement of the identified equipment and materials by the University of California or the U.S. Energy Research and Development Administration to the exclusion of any other equipment or materials made by other manufacturers which may be equally well suited to the purposes of the work reported
28. A. F. Bernhardt: Ph.D. Dissertation, University of California at Davis (June 1975)